

We are IntechOpen, the world's leading publisher of Open Access books Built by scientists, for scientists

5,000

Open access books available

125,000

International authors and editors

140M

Downloads

Our authors are among the

154

Countries delivered to

TOP 1%

most cited scientists

12.2%

Contributors from top 500 universities

**WEB OF SCIENCE™**Selection of our books indexed in the Book Citation Index
in Web of Science™ Core Collection (BKCI)

Interested in publishing with us?
Contact book.department@intechopen.com

Numbers displayed above are based on latest data collected.

For more information visit www.intechopen.com

Numerical Modelling of Fouling Process in EGR System: A Review

*Concepción Paz, Eduardo Suárez, Jesús Vence
and Adrián Cabarcos*

Abstract

In order to combat climate change, the new rigorous standards for pollutant reduction have shone a light on the use of exhaust gas recirculation system in order to minimize the NO_x emissions of vehicles. For this reason, the fouling problem that appears on the exhaust gas recirculation line, caused by the deposition of soot particles and hydrocarbons that are part of the exhaust gas, has become particularly relevant in the last few years. In this field, researches have proposed numerical models in order to estimate and predict the deposit formation and growth. Using various numerical techniques, they intend to determine and reproduce the fouling layer buildup considering the different mechanisms that are involved in the deposit formation. This chapter provides a detailed and comprehensive account of the numerical approaches that have been proposed to analyze the fouling phenomenon that occurs inside the exhaust gas system. The main characteristics of each numerical model, as well as their main strengths and weaknesses, are exposed and evaluated, and their simulation capabilities are examined in detail.

Keywords: EGR, fouling, soot agglomerates, thermophoresis, hydrocarbon condensation, erosion, CFD, numerical simulation

1. Introduction

The Sustainable Development Goals (SDG), known as the 2030 Agenda for Sustainable Development, have been adopted by 193 countries since 2015 [1]. Reducing air pollution, development of sustainable cities, and combating climate change are some of the main goals of this plan of action, and, within that context, the reduction of pollutant emissions from vehicles is an important activity to be faced.

In order to minimize greenhouse gas emissions, vehicle emissions for passenger cars have been regulated worldwide by means of several standards, such as the Euro emission standards in Europe or the Tier standards in the USA [2–4]. These successive standards, which define more stringent acceptable limits for polluting emission and fuel economy, push car manufacturers to use the best technology available for vehicle emission control, and this is one of the biggest technical challenges that the automotive industry faces.

The public concern about diseases derived from air pollution and recent emissions scandals, like *dieselgate*, have shone a light on vehicle emissions, particularly in terms of nitrogen oxides (NO_x) and particulate matter emissions [5, 6].

In this context, since 2014, the EURO 6 emission standard set the emissions limit for nitrogen oxides (NO_x) in 60 and 80 mg/km for gasoline and diesel light-duty vehicles, respectively [7]. This fact has extended the use of techniques like the exhaust gas recirculation (EGR) system, which have proven to be an effective way of reducing NO_x formation. Nowadays, the EGR system is used together with other systems, such as diesel oxidation catalyst (DOC), lean NO_x trap (LNT), or selective catalytic reduction (SCR), to fulfill the NO_x emissions in internal combustion engines [8, 9].

The EGR system, whose main components are the EGR pipe, the EGR valve, and the EGR cooler, is a technique in which a portion of exhaust gas is returned to the intake manifold, reducing the oxygen content inside the cylinder—oxygen-poor environment [10]. Since the NO_x formation is increased in an exponential function with a temperature increase, lower oxygen content of the diluted fresh charge leads to a cooler combustion process that drastically reduces the NO_x formation [11]. To increase its effectiveness, the EGR cooler—a compact heat exchanger that uses engine coolant—is in charge of reducing the exhaust gas temperature prior to entering the combustion chamber [12]. The quantity of EGR is regulated by controlling the EGR valve, which manages the EGR rate required under the different work conditions of the engine.

One of the problems encountered in EGR systems is the fouling of the heat exchanger walls. The carbonaceous soot particles and condensable hydrocarbons derived from the combustion process lead to the formation of a highly porous deposit with low thermal conductivity that can cause the degradation in heat transfer performance in the range of 20–30% [13], as **Figure 1** shows. The accumulation of this unwanted material also causes the increase of the pressure drop along the heat exchanger, adversely affecting the control of the EGR rate and decreasing the fuel efficiency due to the increased pumping work [14]. Under significant fouling conditions, the massive increase of the thickness of the deposit can clog some tubes of the heat exchanger, as **Figure 2** shows, hampering the full normal functioning of the device [15].

In the last few decades, numerous investigations have been focused on the study of the fouling process that takes place on the heat exchanger walls of the EGR system. Numerous attempts in analysis, measurement, and prediction of the deposit have contributed to increase the knowledge of the deposit formation, and many of them have pointed out the complexity of the dynamics of this phenomenon. These

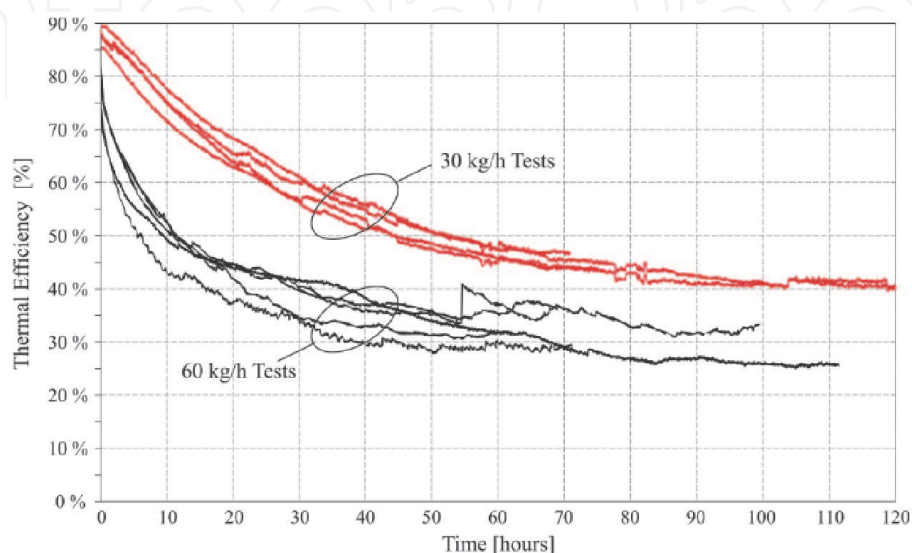


Figure 1. Thermal efficiency evolution of an EGR cooler [16].

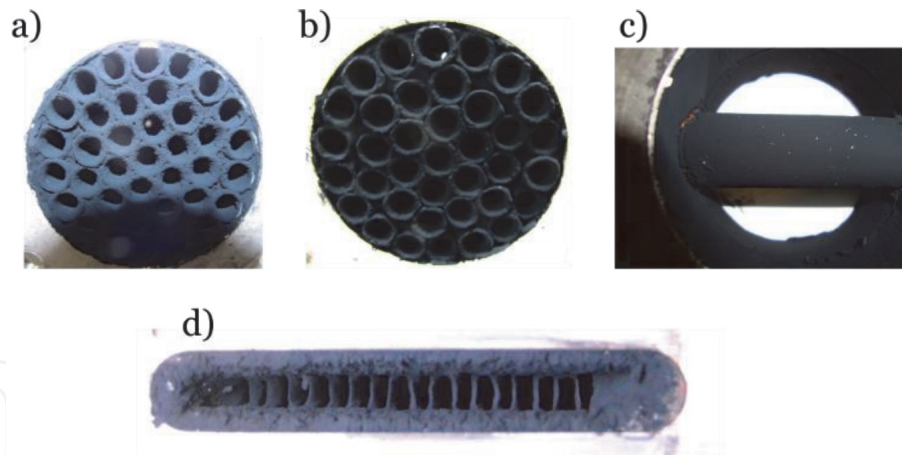


Figure 2.
Photographs of different fouling layers: (a) and (b) show deposits generated by diesel particulate matter inside shell-and-tube heat exchangers, (c) depicts the fouling layer generated on a cylindrical probe which is positioned transverse to the diesel exhaust, and (d) shows the deposit formed by dry soot particles on a tube-and-fin heat exchanger.

studies fall into two broad categories: one group intends to determine and analyze the deposit growth using in situ measurements, i.e., employing experimental procedures to quantify the morphology and characteristics of the fouling layer [17, 18], whereas the second intends to reproduce and recreate the fouling formation employing numerical approaches. The studies of this second category encompass the analysis of the EGR deposit using different numerical models like zero-dimensional (0-D) models, one-dimensional (1-D) models, or advanced computational fluid dynamics (CFD) simulations, which have been created to simulate and reproduce the behavior of the fouling layer that appears inside the EGR technology.

In the following sections, specific features of the different types of numerical approaches used to study the fouling in the EGR system are presented in detail. The functions offered by the several numerical models are examined, and their implementation and results are thoroughly analyzed. In this context, both the composition and characteristics of the particulate matter and the fouling mechanisms involved in this process are briefly presented in advance.

2. Particulate matter involved in EGR fouling

The exhaust gas flow emitted from internal combustion engines has been categorized as dilute flow, where the low concentration of particulate matter (PM) makes negligible the effect of particles on gas flow [19]. Several factors, such as the air-fuel ratio, the EGR rate, the engine load, or the cylinder temperature, can alter the particulate loading in the exhaust flow, and, in the same way, they can influence the formation, agglomeration, and growth of the particles [20].

According to the size of the particulate matter, the nanoparticles emitted from internal combustion engines can be classified into three modes: nucleation, accumulation, and coarse. Nucleation mode is formed by particles that are less than 50 nm in diameter, and, according to the number distribution, most of the particles reside in this mode, as **Figure 3** reports. In the accumulation mode, the agglomerates consist of a collection of much smaller particles, and the size of these aggregates ranges from 50 nm to 1 μm , and particle mass distribution highlights that accumulation mode accounts the largest portion. The biggest particles—diameters between 1 μm and 10 μm —represent only a small fraction of the number of particles, and they belong to the coarse mode [21–23].

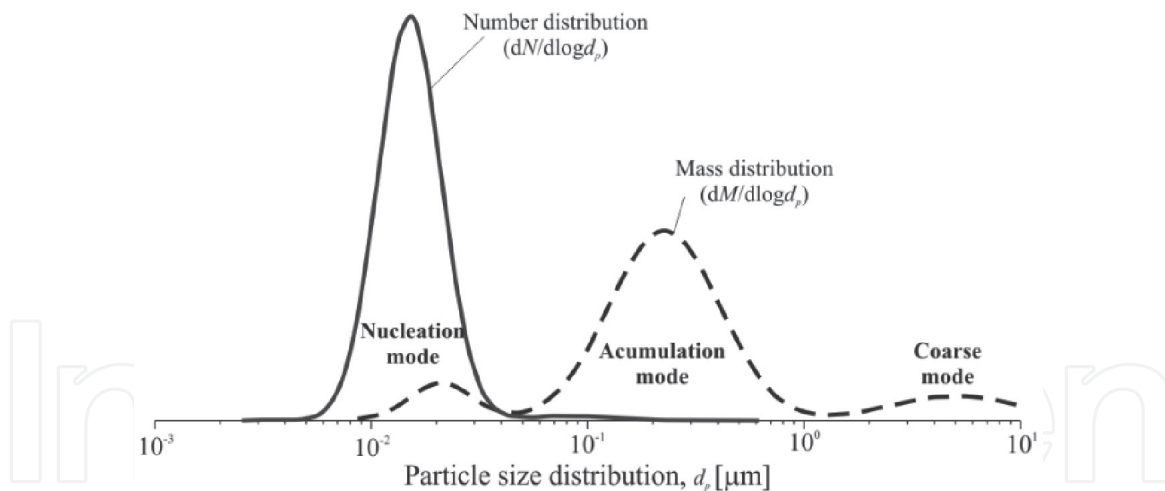


Figure 3.
Generalized size distribution for typical particles emitted by internal combustion engines.

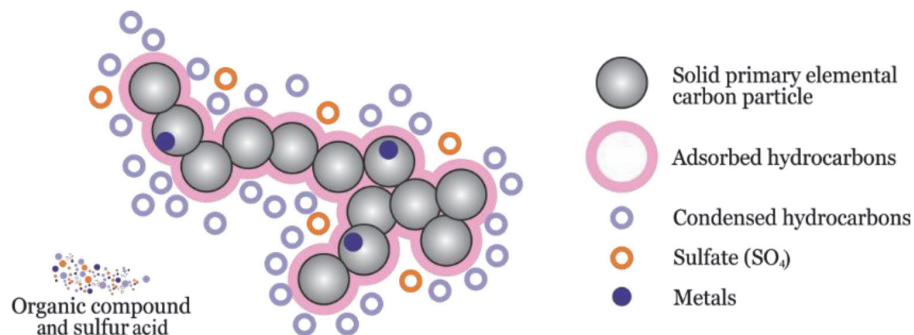


Figure 4.
Agglomerate diesel particle.

Analyzing the composition of the PM of the exhaust gas, the particles are a product of a mix of volatile and nonvolatile species. Volatile fraction is composed by sulfates (SO_4^{2-} + metal sulfate), nitrates (NO_3^- + metal nitrate), and organic elements ($-\text{CH}_2$ + N, O and S). Nonvolatile fraction is composed by carbonaceous particles, commonly referred to as soot, and ash, formed by metals (Fe, Cr, Cu, Zn, Ca) and nonmetals (Si, P, S, Cl) [24]. Several factors, such as fuel and lubricant characteristics or engine work conditions, can influence the composition and proportion of these species, however, in most cases, elemental carbon accounts for around 90% of PM mass [25]. The primary particles—sizes typically between 15 and 30 nm—are composed by carbon and traces of metallic ash, and they aggregate forming complex irregular clusters together with adsorbed and condensed hydrocarbons (HC) [26, 27]. As **Figure 4** shows, the agglomeration of the primary particles causes the formation of clusters with a complex structure with nonuniform shape and compactness [28].

When this particulate matter is deposited on the heat exchanger walls, it forms a fouling layer which coats the heat exchanger surface. The interaction between the particles and the metal surface during the early stages of the deposit formation, and the particle-particle interaction during fouling layer growth, leads to the accumulation of amorphous aggregates on the heat exchanger walls, causing a highly porous deposit (around 98% [18]). This fouling layer, with a complex nanostructure with multiple pores between the deposited aggregates, functions as an insulator between the gas flow and the heat transfer surface. According to the experimental measurements of Lance et al. [18], the fouling layer generated from the deposition of diesel particulate matter has a density around 0.035 g/cm^3 and a low thermal conductivity that is around 0.041 W/mK . However, in some cases, different phenomena, such as

the condensation of hydrocarbons and water or the spallation of the deposit, can collapse the nanostructure of the fouling layer, slightly modifying its thermal properties [20, 29–33]. It is no easy task to determine and quantify the deposit's chemical and physical characteristics due to the fragile nature of the structure, but it is an essential step to provide accurate inputs to the numerical models.

3. Fouling mechanisms in the EGR system

The gas-particle multiphase flow and the formation of fouling layer inside the EGR system are complex phenomena in which several mechanisms are involved. Thermophoresis, diffusion, inertial impact, hydrocarbon condensation, gravitational settling, removal due to shear force, water vapor condensation, or turbulent burst are the main mechanisms that engage in the fouling process.

Excluding the thermal effects, other parameters, such as the particle diffusion, the gravitational settling, the inertial impact of the turbophoresis, play an important role in the EGR fouling formation. The particle diffusion is the dominant mechanism for the small particles, particles with dimensionless relaxation times (t_p^+) less than 0.1, while the transport of large particles, particles with dimensionless relaxation times (τ_p^+) more than 0.1, is dominated by inertial and gravitational effects [34].

Inside the EGR cooler, thermophoresis—induced by the temperature gradient—drives the nanoparticles from the bulk gas flow to the near cool walls, causing the deposition of the soot particles over the heat exchanger surfaces. It has been reported by several authors that under non-isothermal conditions, thermophoresis is the primary mechanism of soot deposition in the particle size typically encountered in exhaust gas, 10 nm to 1 μm , and some correlations from literature, such as Brock-Talbot or Cha-McCoy-Wood, have been used to determine the thermophoretic velocity as a function of the particle diameter [13, 35–38].

The condensation of HC and acids, which are part of the exhaust flow, is significant on a mass basis compared to soot deposition, and it is an important issue in the deposit formation [39]. As exhaust gas is diluted and cooled, the condensation of hydrocarbons is particularly important inside the EGR system. Condensate, which is mixed with soot particles inside the fouling layer, modifies the microstructure of the soot deposit and changes the characteristics of the deposit, leading to an increase of the density and the thermal conductivity of the fouling layer [40].

The effect of shear force of the gas flow over the deposited particles, the turbulent burst, or the water vapor condensation have been identified as potential mechanisms that cause the removal of particles from the fouling layer [41, 42]. When the drag force over the particle is larger than the adhesion force, removal occurs. In the same way, the condensed water droplets can interact with the deposited particles, causing a washout of the dry soot deposit [43].

It has been extensively reported in literature that the formation of the fouling deposits depends on two simultaneous phenomena: the deposition and the removal of particles [13, 44–48]. Such categorization usually selects thermophoresis, particle diffusion, gravitational drift, inertial impact, or hydrocarbon condensation as deposition mechanisms. On the contrary, water vapor condensation, the shear force, or the turbulent burst are usually classified as removal mechanisms.

4. Numerical approaches

In the study of the fouling process of the EGR system, both experimental and numerical investigations have been carried out in order to analyze the effects of the

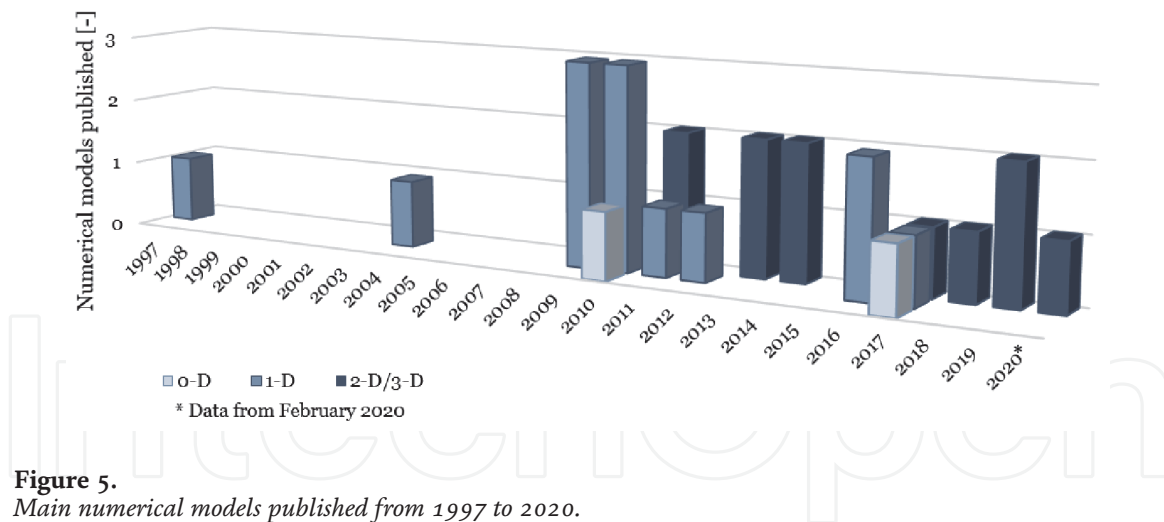


Figure 5.
Main numerical models published from 1997 to 2020.

deposit that grows on the heat exchanger walls. Although the amount of experimental studies have been larger and more frequent, the numerical models have become relevant since 2009, as **Figure 5** depicts, due to the increase in NO_x emission regulation requirements.

The numerical approaches intend to reproduce and simulate the formation and evolution of the deposit inside the EGR system recreating the different mechanisms involved in the fouling process. Because of their significance in the prediction of the deposit, the deposition mechanisms have been implemented in 76.9% of the main numerical models that analyze the deposit formation inside the EGR system. By contrast, the numerical approaches that recreate removal mechanisms are slightly lower (50.0%), and only the 30.8% of the models are focused on the study of the condensation of volatile species. In many cases, several kinds of mechanisms are implemented and coupled in one single numerical approach, in order to achieve more complete simulation frameworks.

According to the complexity of the formulation of the models, they can be divided into three principal categories: the zero-dimensional (0-D), the one-dimensional (1-D), and the multidimensional models.

The zero-dimensional models are focused on an overall heat and material balance of the system, and they do not include any analysis of the fluid dynamics. Following several assumptions and simplifications, they evaluate the overall fouling effects, and, although these numerical approaches avoid any spatial resolution of the variables involved in the process, they can give a fair indication about the fouling phenomenon.

The one-dimensional approach is the next level of complexity. In these models, only one spatial dimension is considered, dividing the fluid zone in different regions and analyzing the properties of the system in each region separately. Although this approach simplifies the number of equations, it can give a detailed evolution of the spatial changes of the fouling parameters.

The multidimensional models require the spatial discretization of the volume of the region and can provide a thorough analysis of the variables of the process. In this field, the use of computational fluid dynamics simulations has been increasing steadily since the 1990s, due to the availability of high-performance computing hardware and the development of user-friendly interfaces. The computer-based simulations make it possible to obtain a detailed solution of the fluid flow, both in two-dimensional (2-D) and three-dimensional (3-D) domains, and they can reproduce the evolution and formation of fouling layers.

5. 0-D models

Table 1 summarizes the 0-D models that have been proposed to analyze the fouling layer effect in the EGR system.

Abarham et al. [49] proposed an analytical model for thermophoretic particle deposition that solves the mass conservation of particles and the energy equation of the gas flow for a single turbulent pipe flow. This approach considers the submicron particle deposition due to the thermophoretic effect, neglecting the diffusion and other deposition mechanisms. The model takes into consideration the pipe diameter reduction due to the growth of the fouling layer and considers different boundary conditions, such as the inlet temperature and mass flow rate of the gas, the inlet particle concentration, or the wall temperature. In this study, the properties of the soot layer, i.e., density, porosity, and thermal conductivity, have been taken from the experimental measurements of Lance et al. [18], and the soot particle diameter has been set at 57 nm, based on the study of Maricq and Harris [51]. This model computes the total mass deposited on the tube and evaluates the degradation of the heat transfer effectiveness over time. To verify the results of this numerical approach, the data were compared with the experimental measurements obtained by the Oak Ridge National Laboratory, and an acceptable agreement was achieved between both methods.

Garrido et al. [50] presented a theoretical analysis of the thermodynamics of exhaust gas condensation. They analyzed the condensation of different species that are part of the exhaust gas produced by gasoline engines, such as water vapor, ammonium, and sulfuric, nitrous, nitric, and chloric acids. The examination of the chemical reactions that takes place along the exhaust line and the analysis of the vapor-liquid equilibrium of the condensable species under different temperatures allow the study of their behavior and the calculation of their dew point. The experimental validation of the model showed that, although the collected condensate amount was slightly lower than the model predicted results, the general tendencies were verified.

Since the 0-D models do not provide any spatial resolution of the fouling parameters, their scope is deliberately more concise. Nevertheless, they can be used as essential tools in guiding the study of the fouling phenomenon.

| Authors | Mechanisms modeled | Main fouling equations | Parameters analyzed | Model—experiment | Remarks |
|---------------------|---|--|--|------------------------------|--|
| Abarham et al. [49] | Thermophoresis | $K_{th} = \frac{2C_p C_c}{1+3C_m K_n} \frac{k_g/k_p + C_i K_n}{1+2k_g/k_p + 2C_i K_n}$ | <ul style="list-style-type: none"> • Deposited soot mass • Cooler effectiveness • Pipe diameter reduction | In reasonable agreement | An analytical solution for thermophoretic deposition of submicron particles |
| Garrido et al. [50] | <ul style="list-style-type: none"> • Water vapor condensation • Acid condensation | $\dot{m}_{cond} = \dot{m}_g (w_{i,initial} - w_{i,end})$ | <ul style="list-style-type: none"> • Saturation temperature • Condensation flux | General tendencies validated | Theoretical analysis of the thermodynamics of gasoline engine exhaust condensation |

Table 1.
0-D model.

6. 1-D models

According to the mechanisms considered by the 1-D models, they can be categorized in five groups, as **Table 2** summarizes. The first group covers those models that only analyze the condensation of water or hydrocarbons. The second group is formed by those studies that investigate the fouling layer formation solely by considering the effect of particle deposition mechanisms. The third group, which combines the characteristic of the two previous groups, contains those models that take into account both the prediction of the HC condensation and the deposition of particulate matter. The fourth group includes those models that, in addition to simulating the particulate matter deposition, also discuss the removal mechanisms. And the fifth group is composed of those investigations that take into consideration all of the mechanisms mentioned above: deposition of particulate matter, removal of particles from the deposit, and condensation of hydrocarbons.

The 1-D models included in the first group are exclusively focused on the analysis of the condensation mechanisms that occur inside the exhaust system. When the temperature of the EGR line drops below the dew point of the condensable species, the condensate—made up of water, HC, and acids—appears. This condensate interacts with the soot-deposited particles, modifying the physical structure of the fouling, and it may corrode the walls of the heat exchanger when the acid amount is high enough.

On the one hand, when the fuel sulfur content is rather high, the detection of the sulfuric acid condensation becomes relevant, and, in this field, McKinley et al. [52] proposed a 1-D model that predicts the condensation of the acid. This numerical approach allows to compute the sulfuric acid dew point considering the coolant temperature, the concentration of the acid, and the engine operating point. The acid condensation rate is calculated assuming that condensate is formed due to direct condensation on the wall and due to formation in a portion of the boundary layer. In addition, the model estimates the condensate composition inside the EGR cooler, taking into account the sulfuric acid and water vapor condensation fluxes. All of these parameters allow the analysis and detection of the sulfuric acid condensation inside the EGR cooler, and, although this is an unvalidated model, it represents an essential step in understanding the effects of the acid condensation on the fouling process.

On the other hand, during the starting of a cold engine—in the first few hundred seconds—the water condensation and evaporation can interact with the existing deposit on the EGR cooler walls and can alter the normal functioning of other exhaust after-treatment devices, such as the catalyst. Although it is a process that occurs mainly during the first few seconds of an engine service, it can cause a severe effect on the deposit evolution. Within this framework, Sharma et al. [53] proposed a 1-D model that simulates the condensation and evaporation of water inside the exhaust line. This is a mathematical model that computes the condensation and evaporation rate of water and that calculates the gas flow temperature considering the heat transfer due to phase change processes. The model provides more accurate simulations of the evolution of the temperature of the gas flow than previous models that do not consider the effect of water condensation and evaporation, and it was validated with experimental results, achieving a high level of agreement.

The second group is formed by the 1-D models that investigate the fouling layer formation solely by considering the effect of soot particle deposition mechanisms. For the sake of simplicity, these numerical approaches intend to compute the fouling buildup taking into account only the effect of particulate matter deposition mechanisms, neglecting both the removal mechanisms and the presence of

| Authors | Mechanisms modeled | Main fouling equations | Parameters analyzed | Model—experiment | Remarks |
|---------------------|---|--|--|----------------------------------|---|
| McKinley [52] | Acid condensation | $\dot{m}_{cond} = \rho_g h A \frac{MW_i}{MW_g} \left(y_i - \frac{P_i(T_s)}{P_g} \right)$ | <ul style="list-style-type: none"> Dew point Condensation flux | — | Prediction of condensation rate and condensate composition to minimize EGR cooler corrosion |
| Sharma et al. [53] | Water vapor condensation | $R_{cond} = k_{cond} y_{water} (1 - \theta)$ $R_{evap} = k_{evap} \theta$ | Condensation evaporation fluxes | Close agreement observed | Simulation of temperature profiles inside after-treatment devices considering water condensation and evaporation |
| B. Ismail [55] | <ul style="list-style-type: none"> Thermophoresis Diffusion | $G_{th} = -2C_s \frac{\left(\frac{k_p + C_t K_n}{1 + 3C_m K_n} \right) [1 + K_n (1.2 + 0.41e^{-0.88K_n})]}{\left(1 + 2\frac{k_p}{k_p} + 2C_t K_n \right)} \frac{\nu_g}{T_g}$ | <ul style="list-style-type: none"> Soot layer thickness Effectiveness degradation Pressure drop evolution | — | Calculation of the coupling between the gas and particle phases to compute the soot deposition in diesel EGR cooling devices |
| Abarham et al. [56] | Thermophoresis | $V_{th} = -K_{th} \frac{\nu_g}{T_g} \vec{\nabla} T$ | <ul style="list-style-type: none"> Tube diameter reduction Soot layer thickness Deposit interface temperature Effectiveness degradation Pressure drop | Significant differences observed | Prediction of EGR cooler fouling amount and distribution across a concentric tube heat exchanger with a constant wall temperature |
| Abarham et al. [57] | <ul style="list-style-type: none"> Thermophoresis HC condensation | $V_{th} = -K_{th} \frac{\nu_g}{T_g} \vec{\nabla} T$ $j_i = K_g \rho_g \ln \left(\frac{y_{interface}}{y_o} \right)$ | <ul style="list-style-type: none"> Tube diameter reduction Deposit interface temperature Mass gain Pressure drop HC condensed mass | Significant differences observed | Simulation of soot and HC deposition on a concentric tube EGR cooler with a constant wall temperature |

| Authors | Mechanisms modeled | Main fouling equations | Parameters analyzed | Model—experiment | Remarks |
|--------------------------------------|---|---|---|---|--|
| Teng and Regner [58] | <ul style="list-style-type: none"> • Thermophoresis • Removal | $\dot{m}_{dep} = K_1 \eta_{dep} U \rho_g C$ $\dot{m}_{rem} = K_2 \rho_g U^2 \delta_d$ | Cooler effectiveness degradation | Good agreement observed | Prediction of the cooler effectiveness deterioration considering the characteristics of the soot deposit |
| Teng and Regner [59] | <ul style="list-style-type: none"> • Thermophoresis • Removal | $\dot{m}_{dep} = K_1 \eta_{dep} U \rho_g C$ $\dot{m}_{rem} = K_2 \rho_g U^2 \delta_d$ | Cooler effectiveness degradation | Good agreement observed | Calculation of soot particle accumulation employing heat, mass, and momentum transfer theories for the particle-gas system |
| Teng [60] | <ul style="list-style-type: none"> • Thermophoresis • Removal | $V_{th} = -K_{th} \frac{v_g}{T_g} \vec{\nabla} T$ $\Delta p = K_f \frac{(\rho_g U)^2}{2\rho_f}$ | <ul style="list-style-type: none"> • Cooler effectiveness degradation • Pressure drop | Good agreement observed | Semiempirical model that predicts cooler effectiveness degradation and pressure drop over fouled EGR coolers |
| Mehravaran and Brereton [61] | <ul style="list-style-type: none"> • Thermophoresis • Diffusion • Removal | $J_r = -(D_B + D_t) \frac{\partial C}{\partial r} + V_{th} C$ $\dot{m}_{rem} = b m_{dep}$ $b \propto \frac{\bar{v}_w}{\varphi}$ | Deposit thickness | Good conformity with literature results | Prediction of soot layer formation based on existing experimental and numerical observations |
| Reza Razmavar and Reza Malayeri [62] | <ul style="list-style-type: none"> • Thermophoresis • Removal • Sticking probability | $V_{th} = -K_{th} \frac{v_g}{T_g} \vec{\nabla} T$ $J_{rem} = K \left(\frac{U}{U_{cr}} \right) \rho_f k_f R_f$ | <ul style="list-style-type: none"> • Fouling thermal resistance • Deposition flux • Removal flux • Total mass deposited | Good agreement observed | Analysis of soot particle deposition and three potential removal mechanisms |
| Sul et al. [63] | <ul style="list-style-type: none"> • Thermophoresis • Removal | $V_{th} = -K_{th} \frac{v_g}{T_g} \vec{\nabla} T$ $\dot{m}_{rem} = \frac{1}{\Delta t A} f(\delta, T, \Delta P, \Delta P^2)$ | <ul style="list-style-type: none"> • Thermal effectiveness • Trapped soot mass • Deposit thickness • Deposit surface temperature • Pressure drop | Good correspondence | Simulation of EGR cooler fouling considering thermophoretic equation and an empirically derived removal function |

| Authors | Mechanisms modeled | Main fouling equations | Parameters analyzed | Model—experiment | Remarks |
|-------------------|--|---|--|---------------------------|--|
| Kuan et al. [64] | <ul style="list-style-type: none"> • Thermophoresis • Removal | $V_{th} = -K_{th} \frac{\nu_g}{T_g} \vec{\nabla} T$ $\text{If } \Delta P < c_0 T_s + c_1$ $\dot{m}_{rem} = 0$ Else : $\dot{m}_{rem} = e^{(c_2 + c_3 T_s + c_4 \delta + c_5 \Delta P)}$ | <ul style="list-style-type: none"> • Exhaust outlet temperature • Fouling factor • Deposit thickness | Close agreement observed | Prediction of the long-term fouling behavior of EGR coolers on a medium-duty diesel engine for steady-state conditions |
| Waley et al. [65] | <ul style="list-style-type: none"> • Thermophoresis • Diffusion • Inertial impaction • Gravitational drift • Removal • HC condensation | $V_{th} = -K_{th} \frac{\nu_g}{T_g} \vec{\nabla} T$ $V_d = 0.057 u^* \left(\frac{3\pi\mu_g^2 d_p}{\rho_g k_b T C_c} \right)^{-\frac{2}{3}}$ $V_i = 4.5 \cdot 10^{-4} u^* \left(\frac{\tau_p u^{*2}}{\nu_g} \right)^2$ $V_g = \left(1 - \frac{\rho_g}{\rho_p} \right) g \tau_p$ $\dot{m}_{rem} = \frac{K \tau_w m_{dep}}{\psi}$ $j_i = K_g \rho_g \ln \left(\frac{y_{interface}}{y_o} \right)$ | <ul style="list-style-type: none"> • Deposit thickness • Condensed HC mass • Deposit surface temperature • Total soot mass • Cooler effectiveness reduction • Fouling thermal resistance | Reasonably good agreement | Calculation of soot deposition, soot removal, and condensation of several HC species in a circular tube with turbulent gas flow at constant wall temperature |

Table 2.
1-D models.

hydrocarbon and water condensates. These simplified models are based on the assumption that thermophoretic effect is three to four orders of magnitude bigger than other deposition mechanisms, and during the first stages of the deposit growth, the removal of particles does not take place [54].

The investigations of B. Ismail [55] and Abarham et al. [56], which proposed 1-D models that investigate the soot deposit evolution considering only the effect of particulate matter deposition mechanisms, are included in this category.

Ismail [55] developed a simplified model, based on two-phase gas-particle conservation equations, which simulates the heat transfer, pressure drop, and soot deposition in EGR cooling devices. This model takes into consideration the particle transport due to the effect of diffusion and thermophoresis and employs a quasi-steady-state formulation that computes the incremental deposited layer thickness along the heat exchanger. It allows the prediction of the change in soot layer thickness, the evolution of the temperature at the outlet of the heat exchanger, and the increase in pressure drop across the EGR cooling device. The weak point of this simplified model is that, although it allows the prediction of the main effects of the soot deposit on the cooler performance, its results were not validated with experimental data.

In the same way, the model presented by Abarham et al. [56] permits to simulate the cooler effectiveness degradation and pressure drop along the EGR cooler, taking into account the particulate matter deposition caused by the thermophoretic effect. This numerical approach allows the calculation of the reduction of the cross sectional area of the tube and estimates the evolution of the temperature of the soot layer interface. In this case, the results of this 1-D model were verified using the experimental measurements of a controlled EGR cooler fouling test, and, although the predicted values for the EGR cooler effectiveness were in agreement with experimental data, the values expected in pressure drop differed significantly from the experimental measurements.

The analysis of the performance of the models of the second group shows that the simulation of the fouling process solely by considering the deposition mechanisms does not bring about the expected results regarding the evolution of the pressure drop along the EGR cooler. As Abarham et al. [56] detailed, although these simplified 1-D models reproduce the fouling growth yielding positive results, it should be expected that the addition of removal mechanisms may improve the predictive capabilities of these models.

In order to complete the features of the abovementioned numerical approach, Abraham et al. [57] added to their model the simulation of the HC condensation, and this new model belongs to the third group, i.e., the category of 1-D models that take into account both the prediction of the HC condensation and the deposition of soot particles. This numerical approach incorporates, coupling with the soot particle deposition equations, the calculation of the dew point and the total mass flux of HC that condenses and becomes part of the deposit. As their other model, it allows to compute the cooler efficiency degradation and the pressure drop evolution neglecting the changes in the physical structure and the chemical reactions that occur in the fouling layer due to the presence of condensate.

Despite the fact that another mechanism was added to the model, the comparison between experimental data and the results of the new model showed a certain mismatch. Although the predicted cooler effectiveness degradation was in agreement with the experimental measurements, the calculated pressure drop continued to display certain differences with the experimental data, and no improvements were seen in this field.

The fourth category comprises the higher number of 1-D numerical approaches, and it covers those models that, in addition to simulating the particulate matter

deposition, also discuss the removal mechanisms. Following the assumption of Kern and Seaton [66], which determined that the net growth of the fouling layer depends on two opposing simultaneous processes of deposition and removal, the models of this category recreate the effects of the fouling deposit on the EGR cooler performance.

The models proposed by Teng and Regner [58, 59], Teng [60], Mehravaran and Brereton [61], Reza Razmavar and Reza Malayeri [62], Sul et al. [63], and Kuan et al. [64] belong to this fourth category. These models compute the deterioration of the heat exchanger effectiveness caused by the fouling layer growth and calculate the increase in pressure drop along the device.

On the one hand, with regard to the particle deposition process, thermophoresis is, in the majority of cases, the only referred deposition mechanism. Although some of these numerical approaches take into consideration the deposition of particulate matter due both to diffusion and thermophoretic effect, such as the model of Mehravaran and Brereton [61], the simulation of the deposition phenomenon of the remaining models is, on an exclusive basis, the calculation of the thermophoretic coefficient.

On the other hand, the removal of soot particles from the deposit is computed using different methodologies. One of these is based on the simulation of the different mechanisms that produce the erosion of the particles, i.e., calculating the physical phenomena that is potentially responsible for the removal of deposited particles. This physical approach, as used by Reza Razmavar and Reza Malayeri [62], simulates removal mechanisms such as the shear force, the effect of incident particle impact, or the particle rolling, allowing to estimate the gas maximum critical velocity to compute the particle removal flux. The other removal approach is quite different, and it is based on empirically derived removal functions that allow the estimation of the removal trend. In this removal approach, as the one proposed by Sul et al. [63], the equation that computes the removal rate is a function of different parameters, such as the deposit thickness, the temperature, or the pressure drop, and it was derived from the data of experimental tests that cover a wide range of fouling conditions.

All numerical models of this fourth category were validated with experimental data. The evolution of the overall parameters of the EGR cooler undergoing a fouling process was compared with the models' results, and, in general, they were in agreement. Although the lack of detailed information prevents a full appraisal of the performance of each mechanism involved in the process, it may be concluded that the combination of deposition and removal mechanisms is expected to provide accurate simulations of the fouling process caused by soot particles.

Finally, the fifth category of 1-D models covers the numerical approaches that take into consideration the deposition mechanisms, the removal mechanisms, and the condensation of hydrocarbons. In addition to the features of the models of the previous group, the approaches of this category include the simulation of the hydrocarbon condensation, implementing the three phenomena in a comprehensive model.

It is worth stressing that, following the methodology of the previous models, the numerical implementations of this category also assume that the deposit, which is formed by soot particles and condensates, has uniform properties. Although, as has been mentioned, the presence of condensate can alter the physical structure of the deposit changing its properties, the density and thermal conductivity of the modeled fouling layer do not change over time, regardless of the amount of condensate expected.

The model proposed by Warey et al. [65] belongs to this fifth category, and it is able to compute the total mass deposited and the fouling layer resistance over time.

The model predictions were validated, and they were in reasonably good agreement with experimental data.

7. Multidimensional models

According to the methodology used to study the fouling process, the multidimensional models can be categorized in five groups, as **Table 3** summarizes. The first category covers those numerical studies that analyze the exhaust gas flow and its effects on the deposit formation, neglecting the simulation of any fouling layer inside the heat exchanger. The second group is formed by those models that, using Eulerian–Lagrangian approach, determine the soot particle deposition on the walls of the EGR system. The third group contains those models that, using a species transport modeling approach, compute the condensation of different hydrocarbons. The fourth category includes those models that intend to reproduce the effects of the deposit, modifying the heat exchange properties of the EGR cooler surface. And the fifth group is composed of those investigations that recreate the real growth of the deposit on the walls of the EGR cooler.

The multidimensional models included in the first category are focused on the analysis of the exhaust gas flow to assess how changes in heat exchanger shape characteristics can reduce or minimize the fouling layer formation. Knowing that, in most cases, the removal process is caused by shear force, these numerical simulations intend on determining which EGR surface structures increase the shear stress and, thus, lead to an effective deposit suppression. Analyzing different parameters, such as the wall shear stress, the velocity field, or the temperature profile along the EGR cooler, these models intend to determine the fouling propensity of several heat exchanger configurations, as Lee and Min [31] and Mohammadi and Malayeri [67] shown.

Since, in the majority of cases, these models are single-phase numerical simulations, where only the gas flow is taken into consideration, the simplicity of these models allow a detailed examination of all the gas parameters involved in the fouling process. Therefore, they provide an exhaustive examination of the gas variables that can be induced or reduce the fouling layer growth. By contrast, these numerical approaches do not bring any information about the fouling mechanisms. They do not provide the estimation of deposited particulate matter, the number of removed particles, or the amount of condensate that will be generated. For this reason, although these models give an initial estimation of the fouling phenomenon, they have a limited scope of application.

The second category is formed by those models that reproduce the soot particle deposition using an Eulerian-Lagrangian approach. Employing the Lagrangian framework, these models track the trajectory of each soot particle in order to determine the regions where they can be deposited. Computing the particle transport equation, which takes into consideration the forces of the gas flow acting on a single particle, these numerical approaches determine the movement of the particulate matter inside the EGR cooler. Considering different soot particle diameters, these models offer an in-depth analysis of the particle deposition and allow the computing of the deposition efficiency inside different EGR cooler configurations.

Just like the models of the previous group, which only analyze the gas phase, the numerical approaches of this category do not provide any information about the growth and evolution of the fouling deposit, and, although they give relevant data about the regions where deposition will occur, they do not reproduce the interaction between the soot deposit and the exhaust gas flow.

| Authors | Mechanisms modeled | Main fouling equations | Parameters analyzed | Model—experiment | Remarks |
|-----------------------------|---|---|--|--|---|
| Lee and Min [31] | — | — | <ul style="list-style-type: none"> Exhaust gas velocity Exhaust gas temperature Exhaust gas pressure | — | Analysis of the gas phase |
| Mohammadi and Malayeri [67] | — | — | Wall shear stress | — | Study of various tube structures that encourage the deposit suppression |
| Xu et al. [68] | <ul style="list-style-type: none"> Thermophoresis Diffusion Inertial impaction | $\frac{du_p}{dt} = \frac{C_d Re_p}{24\tau_p} (u_g - u_p) + \frac{g(\rho_p - \rho_g)}{\rho_p} + F_B + F_S + F_{th}$ | <ul style="list-style-type: none"> Deposition efficiency Deposition velocity Particle deposition distribution | Good conformity with literature results | Simulation of soot particle deposition inside a plate-fin heat exchanger |
| Nagendra et al. [69] | <ul style="list-style-type: none"> Thermophoresis Diffusion | $\frac{du_p}{dt} = F_{drag} + F_{th} + F_{others}$ | <ul style="list-style-type: none"> Forces acting on particles Deposition fraction Exhaust gas velocity | Good conformity with literature results | Calculation of soot particle deposition on wavy-fin EGR coolers |
| Yang et al. [70] | <ul style="list-style-type: none"> Water vapor condensation Acid condensation | $\dot{m}_{cond} \pi d = \frac{\tau_i}{2\nu_{film}} \delta_{film}^2$ | <ul style="list-style-type: none"> Dew point Condensation flux | Close agreement observed with literature results | Prediction of condensation of water vapor, sulfuric acid, and nitric acid formed in the exhaust gases of diesel engines |
| Gonçalves Guedes [71] | <ul style="list-style-type: none"> Deposition Removal Condensation | $V_{th} = -K_{th} \frac{\nu_g}{T_g} \vec{\nabla} T$ $V_d = 0.057u^* \left(\frac{3\pi\mu_g^2 d_p}{\rho_g k_b T C_c} \right)^{-\frac{2}{3}}$ | <ul style="list-style-type: none"> Deposit thickness Deposition efficiency | Differences observed with data from literature | Evaluation of temperature evolution inside a cooler, changing the dependence of the deposit thermal conductivity |

| Authors | Mechanisms modeled | Main fouling equations | Parameters analyzed | Model—experiment | Remarks |
|---------------------|--|--|--|-------------------------|--|
| | | $V_i = 4.5 \cdot 10^{-4} u^* \left(\frac{\tau_p u^{*2}}{\nu_g} \right)^2$ $\log_{10} P_{vap} = AA - \frac{BB}{T_s + CC}$ | <ul style="list-style-type: none"> • Outlet gas temperature • Condensation rate | | |
| Paz et al. [72] | <ul style="list-style-type: none"> • Thermophoresis • Diffusion • Inertial impaction • Removal | $u_{di}^+ = 0.057 Sc^{-\frac{2}{3}} + 4.5 \cdot 10^{-4} \tau_p^{+2}$ $u_{th}^+ = -\frac{2C_i}{1+3C_m K_n} \frac{\frac{k}{k_p} + C_i K_n}{1+2\frac{k}{k_p} + 2C_i K_n} \frac{\nu C_i \nabla T}{u^* T}$ $u_{rem}^+ = \frac{\tau_w \delta_d}{\psi u^*}$ | <ul style="list-style-type: none"> • Deposit thickness evolution • Deposited mass | Good agreement observed | Simulation of the real depth of the fouling layer and its effects on the hydrodynamic of the flow |
| Abarham et al. [73] | <ul style="list-style-type: none"> • Thermophoresis • Diffusion | $\frac{\partial(\rho_g Y)}{\partial t} + \nabla \cdot (\rho_g (\tilde{v} + V_{th}) Y) = \nabla \cdot (\rho_g D_B \nabla Y) + \nabla \cdot (-\rho_g (v'' Y'' + V_{th}'' Y''))$ | <ul style="list-style-type: none"> • Effectiveness degradation • Deposited mass • Deposit thickness | Good agreement observed | 2-D axisymmetric model that computes the growth of the deposit using dynamic grids |
| Paz et al. [74] | <ul style="list-style-type: none"> • Thermophoresis • Diffusion • Inertial impaction • Removal | $\Delta \delta_d = \left(\frac{S_d (u_{di} + u_{th}) C}{\rho_f} - \frac{\tau_w \delta_d}{\psi} \right) \Delta t$ | Deposit thickness | — | 3-D model that computes the fouling layer evolution, considering the movement of the fouling-gas interface |
| Paz et al. [75] | <ul style="list-style-type: none"> • Thermophoresis • Diffusion • Inertial impaction • Removal | $\dot{m}_{dep} = S_d (V_{th} + V_d + V_i) C$ $\dot{m}_{rem} = K \hat{\tau}_w \delta_d$ | <ul style="list-style-type: none"> • Thermal efficiency degradation • Pressure drop • Outlet gas temperature • Deposit thickness | Good agreement observed | Detailed experimental validation of the local fouling thickness |

| Authors | Mechanisms modeled | Main fouling equations | Parameters analyzed | Model—experiment | Remarks |
|-----------------|---|--|---|---|--|
| Paz et al. [76] | <ul style="list-style-type: none"> • Thermophoresis • Diffusion • Inertial impaction • Removal • HC condensation | $\Delta\delta_d = \left(\frac{S_d(u_{di}+u_{th})C}{\rho_f} - \frac{\tau_w\delta_d}{\psi} \right) \Delta t$ $j_i = K_g\rho_g \ln \left(\frac{1-y_i}{1-y_o} \right)$ | <ul style="list-style-type: none"> • Condensation flux • Condensed mass • Deposit surface temperature • Areas where condensation occurs | Good conformity with literature results | Calculation of the HC condensation process considering local scale effects |

Table 3.
 Multidimensional models.

The models proposed by Xu et al. [68] and Nagendra et al. [69] use this technique in order to compute the submicron particle deposition inside plate-and-fin heat exchangers. They evaluated the particle deposition under different boundary conditions and validated their results, achieving a good agreement with the experimental measurements taken from literature.

The third category includes the multidimensional models that use the species transport modeling approach to compute the condensation of different condensable species. Considering convection, diffusion, or even the chemical reactions that take place in the exhaust gas mixture, these numerical approaches compute the partial pressure of each species to determine their dew temperature. The corresponding condensation flux is calculated in the presence of non-condensable gases, and the thin liquid film of condensate that appears on the walls of the heat exchanger is simulated.

An example that uses this modeling approach is the study proposed by Yang et al. [70]. In order to estimate the corrosion inside the EGR system of heavy-duty trucks, they developed a numerical technique that determines the condensation of nitric and sulfuric acid. The model allows the carrying out of three-dimensional simulations, computes the heat and mass transfer processes, and calculates the amount of condensate formed on the heat exchanger walls. Using the Ansys Fluent CFD code, it computes the condensation flux of water vapor, sulfuric acid, and nitric acid, providing results under different operating conditions. Results of this numerical approach were validated, and they were in close agreement with the data from literature.

These kinds of models are based solely on the study of the condensation of acid and hydrocarbon species, generating detailed reports about the condensation process and neglecting the study of the particulate matter deposition and removal processes that occur along the EGR system. For this reason, they are suitable means to find the regions where acid condensation takes place and to detect the zones of the EGR system where corrosion problems may occur.

The fourth category is formed by the numerical models that reproduce the effects of the fouling layer, modifying the heat exchange properties of the wall. Computing the fouling thermal resistance that opposes the cooling of the flow, these numerical approaches allow the simulation of the evolution of the temperature of the gas flow inside the EGR cooler. After resolving the exhaust gas flow inside the EGR cooler, the model calculates the thickness of a virtual fouling layer and adjusts the thermal resistance of the heat exchanger surface, achieving a steady-state solution of the temperature field.

Changing the properties of the virtual fouling layer according to the computed deposit thickness, these models, as the evaluated in the study of Gonçalves Guedes [66], allow the simulation of the evolution of the exhaust gas temperature. However, their main disadvantage is that they provide poor results in the calculation of different parameters, such as the pressure drop along the heat exchanger, because they avoid the simulation of the real growth of the fouling layer inside the tube. That is why employing these models, the simulation of the changes in the hydrodynamics of the exhaust gas flow caused by the fouling layer and the local parameters of the deposit cannot be estimated reliably.

Finally, the models of the fifth category intend to recreate the real growth of the deposit on the walls of the EGR cooler. To that end, they simulate the movement of the fouling-gas interface, after computing the nonuniform thickness of the deposit. Thus, taking into consideration the local-scale effects involved in the fouling phenomenon, these numerical approaches reproduce the real formation of the fouling deposit on the heat exchanger walls, causing the reduction of the cross-sectional area of the tube.

According to the methodology used, the numerical models of this fifth group can be divided into two subcategories: those that convert fluid cells into solid cells and those that use the dynamic mesh methodology to recreate the growth of the fouling layer.

On the one hand, the first subcategory includes those models that, to simulate the growth of the deposit, transform the fluid cells of the domain into fouling cells, as **Figure 6a** illustrates. When the thickness of the fouling layer is larger than the height of the fluid cell, this is converted into a solid cell, and it becomes part of the fouling layer domain. These numerical approaches, as the proposed by Paz et al. [72], couple the gas flow solution and the fouling layer growth and provide a local final thickness of the deposit considering the hydrodynamics of the flow.

On the other hand, to recreate the fouling layer growth, the models of the second subcategory employ the dynamic mesh methodology, as the 2-D axisymmetric model proposed by Abarham et al. [73] or the 3-D model proposed by Paz et al. [74–76]. After the fouling thickness calculation, these numerical approaches adjust the thickness of the deposit moving the fouling-fluid interface, as **Figure 6b** shows. At every time-step of the simulation, they estimate the position of the nodes of the mesh and update the fouling layer domain, allowing the possibility to determine the deposit growth evolution.

As **Figure 7** shows, the main advantage of these numerical approaches is that they simulate the evolution of the fouling layer in a local manner. Considering the local properties of the exhaust gas flow and taking into account the mechanisms involved in the fouling process, they provide a comprehensive solution of the fouling layer and recreate its real growth inside the heat exchanger. In contrast, these kinds of models have higher computational costs than other multidimensional

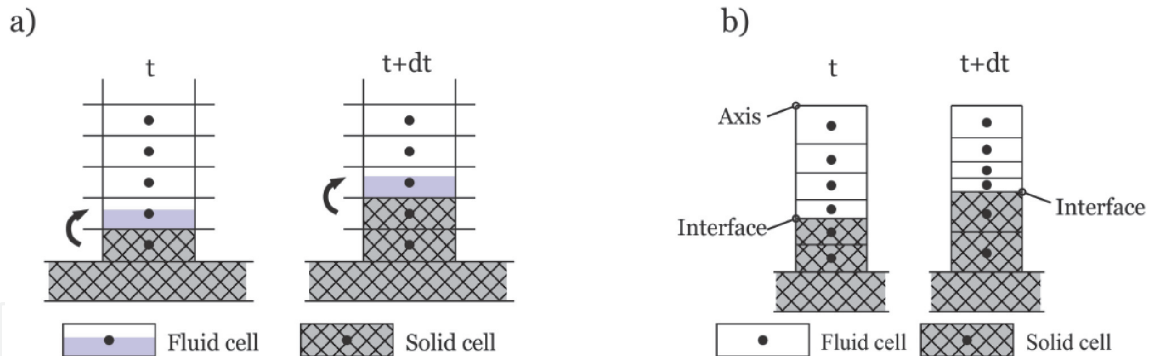


Figure 6. Scheme of the fouling growth: (a) converting fluid cells into solid cells and (b) using the dynamic mesh methodology.

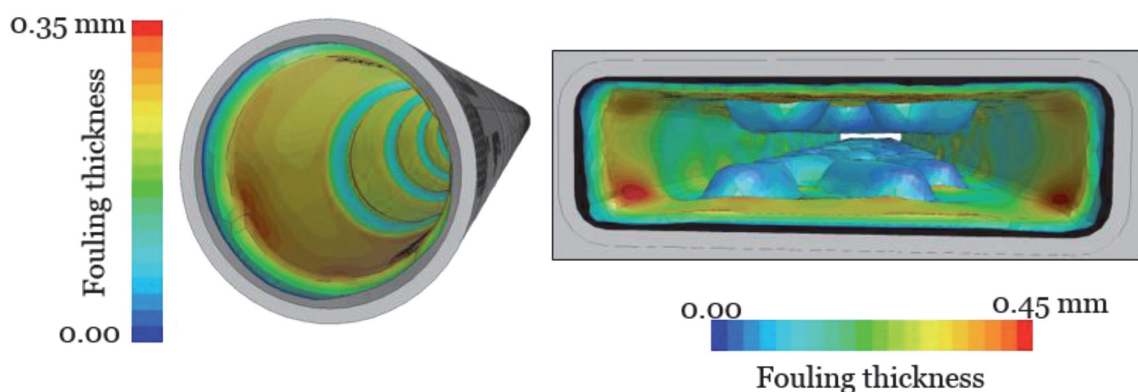


Figure 7. Fouling thickness computed using dynamic mesh methodology.

models, and, although they provide detailed information about the fouling phenomenon, they demand more computational resources.

8. Concluding remarks

This chapter compiles and analyzes the main numerical approaches that have been proposed to predict and reproduce the fouling phenomenon that takes place inside the EGR system. Features of each option, its range of applicability, as well as their main strengths and weaknesses have been highlighted. The fouling prediction capabilities of each numerical approach have been analyzed in detail with the aim of reviewing the most relevant numerical approaches used in the study of the fouling process that occurs in the EGR system.

The stringent construction requirements of new EGR technologies and the development of new numerical techniques, and more particularly the use of computational fluid dynamics codes, have contributed to the creation of more sophisticated models that allow the simulation of the fouling phenomenon considering a large number of parameters and mechanisms. Nevertheless, the simulation of the deposit formation and evolution involves intricate matters, such as the particle-fluid interaction, agglomerate formation, or the physicochemical reactions that take place inside the deposit, which make the fouling process a complex phenomenon that needs to be addressed coherently across all its parameters.

The information and knowledge about the numerical modeling of the fouling process in the EGR system collected in this study may help EGR designers and manufactures to improve and develop new vehicle emissions control techniques, which contribute to meet the Sustainable Development Goals.

Acknowledgements

The authors are grateful for the financial support from the Spanish Ministry of Economy, Industry, and Competitiveness through the ENE2017-87855-R project.

Nomenclature

| | |
|-----------|--|
| 0-D | zero-dimensional |
| 1-D | one-dimensional |
| 2-D | two-dimensional |
| 3-D | three-dimensional |
| A | surface area |
| AA | Antoine coefficient |
| BB | Antoine coefficient |
| CC | Antoine coefficient |
| C | soot concentration |
| c_{0-5} | constant coefficients |
| CFD | computational fluid dynamics |
| C_c | Stokes-Cunningham slip correction factor |
| C_D | drag coefficient |
| C_m | thermophoretic constant |
| C_s | thermophoretic constant |
| C_t | thermophoretic constant |
| D_B | molecular diffusivity |

| | |
|------------|--|
| d | tube diameter |
| d_p | particle diameter |
| D_t | mean effect of velocity and concentration fluctuations |
| DOC | diesel oxidation catalyst |
| EGR | exhaust gas recirculation |
| F_B | Brownian force |
| F_{drag} | drag force |
| F_S | Saffman lift force |
| F_{th} | thermophoretic force |
| g | gravitational acceleration |
| G_{th} | dimensional thermophoretic parameter |
| h | mass transfer coefficient |
| HC | hydrocarbon |
| J | mass flux |
| j_i | mass condensation flux of the i th species |
| K | proportionality constant |
| K_1 | cooler structure-related parameter |
| K_2 | parameter characterizing the dispersion of the soot particles removed from the deposit |
| k_{cond} | condensation rate constant |
| k_{evap} | evaporation rate constant |
| K_f | overall pressure loss factor |
| k_f | fouling layer thermal conductivity |
| K_g | mass transfer coefficient |
| k_g | gas thermal conductivity |
| K_n | Knudsen number |
| k_p | particulate matter thermal conductivity |
| K_{th} | thermophoretic coefficient |
| LNT | lean NOx trap |
| m | mass |
| \dot{m} | mass flow |
| MW | molecular weight |
| NOx | nitrogen oxides |
| P_g | pressure of the gas flow |
| P_i | vapor pressure of the i th species |
| P_{sat} | saturation pressure |
| P_{vap} | vapor pressure |
| PM | particulate matter |
| R_{cond} | condensation rate |
| R_{evap} | evaporation rate |
| R_f | fouling resistance |
| Re_p | particles' Reynolds number |
| SCR | selective catalytic reduction |
| SDG | sustainable development goals |
| S_d | particle sticking probability |
| T_g | gas temperature |
| T_s | surface temperature |
| U | mean velocity |
| U_{C_r} | critical velocity |
| u^* | friction velocity |
| u_{di} | isothermal deposition velocity |
| u_{di}^+ | dimensionless isothermal deposition velocity |


| | |
|-----------------|--|
| u_{th} | thermophoretic deposition velocity |
| u_{th}^+ | dimensionless thermophoretic deposition velocity |
| u_{rem}^+ | dimensionless removal velocity |
| u_g | gas velocity |
| u_p | particle velocity |
| \tilde{v} | time average velocity vector |
| V_d | drift velocity due to diffusion |
| V_g | gravitational drift velocity |
| V_i | drift velocity due to inertial impaction |
| V_{th} | thermophoretic drift velocity |
| Y | particle mass fraction |
| y_i | mole fraction of the i th species |
| $y_{interface}$ | mole fraction of vapor at interface |
| y_o | mole fraction of vapor in bulk mixture |
| w_i | mass fraction of the i th species |
| Greek | |
| δ_d | deposit thickness |
| δ_{film} | liquid film thickness |
| η_{dep} | deposition efficiency |
| θ | fractional surface coverage of water |
| μ_g | gas dynamic viscosity |
| ν_g | gas kinematic viscosity |
| ν_{film} | kinematic viscosity of the liquid film |
| ρ_f | fouling density |
| ρ_g | gas density |
| τ_i | liquid-gas interface shear stress |
| τ_p | particle relaxation time |
| τ_p^+ | dimensionless particle relaxation time |
| τ_w | wall shear stress |
| $\hat{\tau}_w$ | normalized wall shear stress |
| φ | surface bonding force |
| ψ | strength of deposit |

Author details

Concepción Paz*, Eduardo Suárez, Jesús Vence and Adrián Cabarcos
CINTEXT, Universidade de Vigo, Vigo, España

*Address all correspondence to: cpaz@uvigo.es

IntechOpen

© 2020 The Author(s). Licensee IntechOpen. This chapter is distributed under the terms of the Creative Commons Attribution License (<http://creativecommons.org/licenses/by/3.0>), which permits unrestricted use, distribution, and reproduction in any medium, provided the original work is properly cited. 

References

- [1] G. Assembly. Resolution adopted by the General Assembly on 19 September 2016. A/RES/71/1, 3 October 2016 (The New York Declaration); 2010
- [2] Anenberg SC, Miller J, Minjares R, Du L, Henze DK, Lacey F, et al. Impacts and mitigation of excess diesel-related NO_x emissions in 11 major vehicle markets. *Nature*. 2017;**545**(7655):467–471. DOI: 10.1038/nature22086
- [3] Joshi A. Review of vehicle engine efficiency and emissions. In: SAE Technical Paper Series. 2019. DOI: 10.4271/2019-01-0314
- [4] Vestreng V, Ntziachristos L, Semb A, Reis S, Isaksen ISA, Tarrasón L. Evolution of NO_x emissions in Europe with focus on road transport control measures. *Atmospheric Chemistry and Physics*. 2009;**9**(4):1503–1520. DOI: 10.5194/acp-9-1503-2009
- [5] Rissler J, Swietlicki E, Bengtsson A, Boman C, Pagels J, Sandström T, et al. Experimental determination of deposition of diesel exhaust particles in the human respiratory tract. *Journal of Aerosol Science*. 2012;**48**:18–33. DOI: 10.1016/j.jaerosci.2012.01.005
- [6] Brand C. Beyond ‘Dieselgate’: Implications of unaccounted and future air pollutant emissions and energy use for cars in the United Kingdom. *Energy Policy*. 2016;**97**:1–12. DOI: 10.1016/j.enpol.2016.06.036
- [7] May J, Favre C, Bosteels D. Emissions from Euro 3 to Euro 6 light-duty vehicles equipped with a range of emissions control technologies. In: *Internal Combustion Engines: Performance, Fuel Economy and Emissions*. London: Elsevier; 2013. pp. 55–65. DOI: 10.1533/9781782421849.2.55
- [8] Jacobs T, Assanis D, Filipi Z. The Impact of Exhaust Gas Recirculation on Performance and Emissions of a Heavy-Duty Diesel Engine. In: SAE 2003 World Congress & Exhibition. Detroit, Michigan, USA: SAE Technical Paper; 3–6 March 2003. DOI: 10.4271/2003-01-1068
- [9] Deppenkemper K, Lng ME, Schoenen M, Koetter M. Super ultra-low NO_x emissions under extended RDE conditions - evaluation of light-off strategies of advanced diesel exhaust aftertreatment systems. In: SAE Technical Paper Series. 2019. DOI: 10.4271/2019-01-0742
- [10] Wei H, Zhu T, Shu G, Tan L, Wang Y. Gasoline engine exhaust gas recirculation – A review. *Applied Energy*. 2012;**99**:534–544. DOI: 10.1016/j.apenergy.2012.05.011
- [11] Agarwal D, Singh SK, Agarwal AK. Effect of exhaust gas recirculation (EGR) on performance, emissions, deposits and durability of a constant speed compression ignition engine. *Applied Energy*. 2011;**88**(8):2900–2907. DOI: 10.1016/j.apenergy.2011.01.066
- [12] Resitoglu IA. NO_x pollutants from diesel vehicles and trends in the control technologies. In: Richard Viskup, editor. *Diesel and Gasoline Engines*. IntechOpen; 2018.
- [13] Hoard J, Abarham M, Styles D, Giuliano JM, Sluder CS, Storey JME. Diesel EGR cooler fouling. *SAE International Journal of Engines*. 2008; **1**(1):1234–1250. DOI: 10.4271/2008-01-2475
- [14] Ismail BI, Zhang R, Ewing D, Cotton JS, Chang J-S. The heat transfer characteristics of exhaust gas recirculation (EGR) cooling devices. In: *Proceedings of the ASME 2002 International Mechanical Engineering Congress and Exposition*. Vol. 7.

New Orleans, Louisiana, USA: ASME; 17-22 November 2002. p. 539-546. DOI: 10.1115/imece2002-39559

[15] Kim HM, Park SK, Choi K-S, Wang H-M, Lee DH, Lee DK, et al. Investigation on the flow and heat transfer characteristics of diesel engine EGR coolers. *International Journal of Automotive Technology*. 2008;**9**(2): 149–153. DOI: 10.1007/s12239-008-0019-4

[16] Paz C, Suárez E, Eiris A, Porteiro J. Experimental evaluation of the critical local wall shear stress around cylindrical probes fouled by diesel exhaust gases. *Experimental Thermal and Fluid Science*. 2012;**38**:85–93. DOI: 10.1016/j.expthermflusci.2011.11.011

[17] Abarham M, Chafekar T, Hoard JW, Salvi A, Styles DJ, Sluder CS, et al. In-situ visualization of exhaust soot particle deposition and removal in channel flows. *Chemical Engineering Science*. 2012;**87**:359–370. DOI: 10.1016/j.ces.2012.09.025

[18] Lance MJ, Sluder CS, Wang H, Storey JME. Direct Measurement of EGR Cooler Deposit Thermal Properties for Improved Understanding of Cooler Fouling. In: *SAE 2009 World Congress & Exhibition*. Detroit, Michigan, USA: SAE Technical Paper; 20-23 April 2009. DOI: 10.4271/2009-01-1461

[19] Elghobashi S. On predicting particle-laden turbulent flows. *Applied Scientific Research*. 1994;**52**(4):309–329. DOI: 10.1007/bf00936835

[20] Teng H, Barnard M. Physicochemical characteristics of soot deposits in EGR coolers. In: *SAE Technical Papers*. 2010. DOI: 10.4271/2010-01-0730

[21] Bika AS, Warey A, Long D, Balestrino S, Szymkowicz P. Characterization of soot deposition and particle nucleation in exhaust gas recirculation coolers. *Aerosol Science*

and Technology. 2012;**46**(12):1328–1336. DOI: 10.1080/02786826.2012.712730

[22] Eastwood P. *Particulate Emissions from Vehicles*. Chichester: John Wiley and Sons Ltd; 2008

[23] Lapuerta M, Armas O, Gómez A. Diesel particle size distribution estimation from digital image analysis. *Aerosol Science and Technology*. 2003;**37**(4):369–381. DOI: 10.1080/02786820300970

[24] Raza M, Chen L, Leach F, Ding S. A review of particulate number (PN) emissions from gasoline direct injection (GDI) engines and their control techniques. *Energies*. 2018;**11**(6):1417. DOI: 10.3390/en11061417

[25] Fushimi A, Kondo Y, Kobayashi S, Fujitani Y, Saitoh K, Takami A, et al. Chemical composition and source of fine and nanoparticles from recent direct injection gasoline passenger cars: Effects of fuel and ambient temperature. *Atmospheric Environment*. 2016;**124**:77–84. DOI: 10.1016/j.atmosenv.2015.11.017

[26] Maricq MM. Chemical characterization of particulate emissions from diesel engines: A review. *Journal of Aerosol Science*. 2007;**38**(11):1079–1118. DOI: 10.1016/j.jaerosci.2007.08.001

[27] Myung CL, Park S. Exhaust nanoparticle emissions from internal combustion engines: A review. *International Journal of Automotive Technology*. 2011;**13**(1):9–22. DOI: 10.1007/s12239-012-0002-y

[28] Brasil AM, Farias TL, Koylu UO, Carvalho MG. A recipe for image characterization of fractal-like aggregates. *Journal of Aerosol Science*. 1998;**29**:S1275–S1276. DOI: 10.1016/s0021-8502(98)90820-5

[29] Hong K, Park J, Lee K. Experimental evaluation of SOF effects on EGR cooler

fouling under various flow conditions. *International Journal of Automotive Technology*. 2011;**12**(6):813–820. DOI: 10.1007/s12239-011-0093-x

[30] Lance MJ, Sluder S, Lewis S, Storey J. Characterization of field-aged EGR cooler deposits. *SAE International Journal of Engines*. 2010;**3**(2):126–136. DOI: 10.4271/2010-01-2091

[31] Lee J, Min K. A study of the fouling characteristics of EGR coolers in diesel engines. *Journal of Mechanical Science and Technology*. 2014;**28**(8):3395–3401. DOI: 10.1007/s12206-014-0752-8

[32] Lee Y, Hong KS, Song S, Chun KM, Lee KS, Min S, et al. Evaluation of SOF effects on deposit characteristics of the EGR cooler using a PM generator. In: *SAE Technical Papers*. 2011. DOI: 10.4271/2011-01-1156

[33] Salvi A, Hoard J, Bieniek M, Abarham M, Styles D, Assanis D. Effect of volatiles on soot based deposit layers. *Journal of Engineering for Gas Turbines and Power*. 2014;**136**(11):111401. DOI: 10.1115/1.4027460

[34] Young J, Leeming A. A theory of particle deposition in turbulent pipe flow. *Journal of Fluid Mechanics*. 1997; **340**:129–159. DOI: 10.1017/s0022112097005284

[35] Abarham M, Hoard J, Assanis D, Styles D, Curtis EW, Ramesh N. Review of soot deposition and removal mechanisms in EGR coolers. *SAE International Journal of Fuels and Lubricants*. 2010;**3**(1):690–704. DOI: 10.4271/2010-01-1211

[36] Chunhong He GA. Particle deposition with thermophoresis in laminar and turbulent duct flows. *Aerosol Science and Technology*. 1998; **29**(6):525–546. DOI: 10.1080/02786829808965588

[37] Epstein N. Elements of particle deposition onto nonporous solid

surfaces parallel to suspension flows. *Experimental Thermal and Fluid Science*. 1997;**14**(4):323–334. DOI: 10.1016/S0894-1777(96)00135-5

[38] Talbot L, Cheng RK, Schefer RW, Willis DR. Thermophoresis of particles in a heated boundary layer. *Journal of Fluid Mechanics*. 1980;**101**(4):737–758. DOI: 10.1017/s0022112080001905

[39] Mulenga MC, Chang DK, Tjong JS, Styles D. Diesel EGR cooler fouling at freeway cruise. In: *SAE Technical Paper Series*. 2009. DOI: 10.4271/2009-01-1840

[40] Lance MJ, Storey J, Sluder CS, Meyer Iii H, Watkins B, Kaiser M, et al. Microstructural analysis of deposits on heavy-duty EGR coolers. In: *SAE Technical Papers*. Vol. 2. 2013. DOI: 10.4271/2013-01-1288

[41] Cleaver JW, Yates B. Mechanism of detachment of colloidal particles from a flat substrate in a turbulent flow. *Journal of Colloid and Interface Science*. 1973;**44**(3):464–474. DOI: 10.1016/0021-9797(73)90323-8

[42] Warey A, Bika AS, Long D, Balestrino S, Szymkowicz P. Influence of water vapor condensation on exhaust gas recirculation cooler fouling. *International Journal of Heat and Mass Transfer*. 2013;**65**(0):807–816. DOI: 10.1016/j.ijheatmasstransfer.2013.06.063

[43] Warey A, Bika AS, Vassallo A, Balestrino S, Szymkowicz P. Combination of pre-EGR cooler oxidation catalyst and water vapor condensation to mitigate fouling. *SAE International Journal of Engines*. 2014; **7**(1):21–31. DOI: 10.4271/2014-01-0636

[44] Abd-Elhady MS, Malayeri MR. Asymptotic characteristics of particulate deposit formation in exhaust gas recirculation (EGR) coolers. *Applied Thermal Engineering*. 2013;**60**(1–2):96–104. DOI: 10.1016/j.applthermaleng.2013.06.038

- [45] Epstein N. Particulate fouling of heat transfer surfaces: Mechanisms and models. In: Melo LF, Boot TR, Bernardo CA, editors. *Fouling Science and Technology*. Dordrecht: Springer; 1988. pp. 143-164. DOI: 10.1007/978-94-009-2813-8_10
- [46] Freeman WB, Middis J, Müller-Steinhagen HM. Influence of augmented surfaces and of surface finish on particulate fouling in double pipe heat exchangers. *Chemical Engineering and Processing: Process Intensification*. 1990;27(1):1-11. DOI: 10.1016/0255-2701(90)85001-K
- [47] Paz C, Suárez E, Concheiro M, Porteiro J. Experimental study of soot particle fouling on ribbed plates: Applicability of the critical local wall shear stress criterion. *Experimental Thermal and Fluid Science*. 2013;44(0):364-373. DOI: 10.1016/j.expthermflusci.2012.07.008
- [48] Tang S-Z, Wang F-L, Ren Q, He Y-L. Fouling characteristics analysis and morphology prediction of heat exchangers with a particulate fouling model considering deposition and removal mechanisms. *Fuel*. 2017;203:725-738. DOI: 10.1016/j.fuel.2017.03.049
- [49] Abarham M, Hoard J, Assanis D, Styles D, Sluder C, Storey J. An analytical study of thermophoretic particulate deposition in turbulent pipe flows. *Aerosol Science and Technology*. 2010;44(44):785-795. DOI: 10.1080/02786826.2010.491841
- [50] Garrido Gonzalez N, Baar R, Drueckhammer J, Kaepfner C. The thermodynamics of exhaust gas condensation. *SAE International Journal of Engines*. 2017;10(4):1411-1421. DOI: 10.4271/2017-01-9281
- [51] Harris SJ, Maricq MM. The role of fragmentation in defining the signature size distribution of diesel soot. *Journal of Aerosol Science*. 2002;33(6):935-942. DOI: 10.1016/S0021-8502(02)00045-9
- [52] McKinley TL. Modeling sulfuric acid condensation in diesel engine EGR coolers. In: *SAE Technical Papers*. 1997. DOI: 10.4271/970636
- [53] Sharma M, Laing P, Son S. Modeling water condensation in exhaust A/T devices. In: *SAE Technical Paper Series*. 2010. DOI: 10.4271/2010-01-0885
- [54] Housiadas C, Drossinos Y. Thermophoretic deposition in tube flow. *Aerosol Science and Technology*. Apr. 2005;39(4):304-318. DOI: 10.1080/027868290931069
- [55] Ismail B. The Heat Transfer and the Soot Deposition Characteristics in Diesel Engine Exhaust Gas Recirculation Cooling Devices [thesis]. Hamilton: McMaster University; 2004
- [56] Abarham M, Hoard J, Assanis D, Styles D, Curtis EW, Ramesh N, et al. Numerical modeling and experimental investigations of EGR cooler fouling in a diesel engine. In: *SAE 2009 World Congress & Exhibition*. Detroit, Michigan, USA: SAE Technical Paper; 20-23 April 2009. DOI: 10.4271/2009-01-1506
- [57] Abarham M, Hoard J, Assanis DN, Styles D, Curtis EW, Ramesh N, et al. Modeling of thermophoretic soot deposition and hydrocarbon condensation in EGR coolers. *SAE International Journal of Fuels and Lubricants*. 2009;2:921-931. DOI: 10.4271/2009-01-1939
- [58] Teng H, Regner G. Characteristics of soot deposits in EGR coolers. *Society of Automotive Engineers*. 2009;01-2671(2):81-90. DOI: 10.4271/2009-01-2671
- [59] Teng H, Regner G. Particulate fouling in EGR coolers. *SAE International Journal of Commercial Vehicles*. 2010;2(2):154-163. DOI: 10.4271/2009-01-2877

- [60] Teng H. A semi-empirical model for predicting pressure drops of fouled EGR coolers. *SAE International Journal of Commercial Vehicles*. 2010;**3**(1):156–163. DOI: 10.4271/2010-01-1948
- [61] Mehravaran M, Brereton G. Modeling of Thermophoretic Soot Deposition and Stabilization on Cooled Surfaces. In: *Commercial Vehicle Engineering Congress*. Rosemont, Chicago, Illinois, USA: SAE Technical Paper; 13-14 September 2011. DOI: 10.4271/2011-01-2183
- [62] Reza Razmavar A, Reza Malayeri M. A simplified model for deposition and removal of soot particles in an exhaust gas recirculation cooler. *Journal of Engineering for Gas Turbines and Power*. 2016;**138**(1):011505. DOI: 10.1115/1.4031180
- [63] Sul H, Han T, Bieniek M, Hoard J, Kuan C-K, Styles D. The effects of temperature, shear stress, and deposit thickness on EGR cooler fouling removal mechanism - part 2. *SAE International Journal of Materials and Manufacturing*. 2016;**9**(2016–01–0186): 245–253. DOI: 10.4271/2016-01-0186
- [64] Kuan C-K, Styles D, Bieniek M, Hoard J. An EGR cooler fouling model: Experimental correlation and model uses. *SAE International Journal of Engines*. 2017;**10**(2):541–549. DOI: 10.4271/2017-01-0535
- [65] Warray A, Balestrino S, Szymkowitz P, Malayeri MR. A one-dimensional model for particulate deposition and hydrocarbon condensation in exhaust gas recirculation coolers. *Aerosol Science and Technology*. 2012;**46**(2):198–213. DOI: 10.1080/02786826.2011.617400
- [66] Kern DQ, Seaton RE. A theoretical analysis of thermal surface fouling. *British Chemical Engineering*. 1959; **4**(5):258–262
- [67] Mohammadi K, Malayeri MR. Model-based performance of turbulence induced structures in exhaust gas recirculation (EGR) coolers. *Heat Transfer Engineering*. 2014;**36**(7–8): 706–714. DOI: 10.1080/01457632.2015.954949
- [68] Xu Z, Sun A, Han Z, Yu X, Zhang Y. Simulation of particle deposition in a plate-fin heat exchanger using a particle deposition model with a random function method. *Powder Technology*; 2019;**355**:145–156. DOI: 10.1016/j.powtec.2019.07.031
- [69] Nagendra K, Tafti DK, Viswanathan AK. Modeling of soot deposition in wavy-fin exhaust gas recirculator coolers. *International Journal of Heat and Mass Transfer*. 2011; **54**(7–8):1671–1681. DOI: 10.1016/j.ijheatmasstransfer.2010.10.033
- [70] Yang B-J, Mao S, Altin O, Feng Z-G, Michaelides EE. Condensation analysis of exhaust gas recirculation system for heavy-duty trucks. *Journal of Thermal Science and Engineering Applications*. 2011;**3**(4):041007. DOI: 10.1115/1.4004745
- [71] Golçalves Guedes de Pinho Guerra, Sara Raquel. *Fouling of Exhaust Gas Recirculation Coolers* [thesis]. Porto: Universidade do Porto; 2017
- [72] Paz C, Suárez E, Eirís A, Porteiro J. Development of a predictive CFD fouling model for diesel engine exhaust gas systems. *Heat Transfer Engineering*. 2013;**34**(8–9):674–682. DOI: 10.1080/01457632.2012.738321
- [73] Abarham M, Zamankhan P, Hoard JW, Styles D, Sluder CS, Storey JME, et al. CFD analysis of particle transport in axi-symmetric tube flows under the influence of thermophoretic force. *International Journal of Heat and Mass Transfer*. 2013;**61**(0):94–105. DOI: 10.1016/j.ijheatmasstransfer.2013.01.071

[74] Paz C, Suárez E, Conde M, Vence J. Development of a computational fluid dynamics model for predicting fouling process using dynamic mesh model. *Heat Transfer Engineering*. 2020;**41**(2): 199-207. DOI: 10.1080/01457632.2018.1522108

[75] Paz C, Suárez E, Vence J, Cabarcos A. Fouling evolution on ribbed surfaces under EGR dry soot conditions: Experimental measurements and 3D model validation. *International Journal of Thermal Sciences*. 2020;**151**:106271. DOI: 10.1016/j.ijthermalsci.2020.106271

[76] Paz C, Suárez E, Vence J, Gil C. CFD study of the fouling layer evolution due to soot deposition and hydrocarbon condensation inside an exhaust gas recirculation cooler. In: 13th International Conference on Heat Exchanger Fouling and Cleaning. 2019